(2) Sibling donors might be also affected with FA.
(3) Conventional myeloablative conditioning regimens increase the regimen-related mortality.
(4) Higher potential risk of secondary malignancies following HSCT because of the genetic background.

In conclusion, for practical hematologists who manage young adult patients with severe AA, FA must be actively ruled out, particularly in patients between the ages of 20 and 40 years, who are the best candidates for unrelated allo-HSCT using minimal myeloablative conditioning.

Conflict of interest

The authors declare no conflict of interest.

K Maekawa[1], M Yoshimitsu[1], H Fujiwara[1,5], K Matsushita[1], H Kawada[1], H Hamada[1], S Suzuki[1,2], K Uozumi[1,2], M Ohtsuka[3], S Hanada[3], M Yabe[4], H Yabe[4] and N Arima[1,2]

[1]*Department of Hematology and Immunology, Kagoshima University Hospital, Kagoshima, Japan;*
[2]*Division of Hematology and Immunology, Graduate School of Medical and Dental Sciences, Kagoshima University, Kagoshima, Japan;*
[3]*Department of Internal Medicine, National Hospital Organization Kagoshima Medical Center, Kagoshima, Japan and*
[4]*Department of Cell Transplantation and Regenerative Medicine, Tokai University School of Medicine, Kanagawa, Japan*
[5]*Current address: Department of Bioregulatory Medicine, Ehime University Graduate School of Medicine, c/o Department of Cell proliferation and Cancer regulation, Proteomedicine Reserch Center, Toh-on city, Ehime, Japan*
E-mail: nao@m2.kufm.kagoshima-u.ac.jp

References

1 Berger R, Bernheim A, Gluckman E, Gisselbrecht C. *In vitro* effect of cyclophosphamide metabolites on chromosomes of Fanconi anaemia patients. *Br J Haematol* 1980; **45**: 565–568.
2 Alter BP. Diagnosis, genetics, and management of inherited bone marrow failure syndromes. *Hematology Am Soc Hematol Educ Program* 2007, 29–39.
3 Giampietro PF, Adler-Brecher B, Verlander PC, Pavlakis SG, Davis JG, Auerbach AD. The need for more accurate and timely diagnosis in Fanconi anemia: a report from the International Fanconi Anemia Registry. *Pediatrics* 1993; **91**: 1116–1120.
4 Sasaki MS, Tonomura A. A high susceptibility of Fanconi's anemia to chromosome breakage by DNA cross-linking agents. *Cancer Res* 1973; **33**: 1829–1836.
5 Shimamura A, Montes de Oca R, Svenson JL, Haining N, Moreau LA, Nathan DG *et al.* A novel diagnostic screen for defects in the Fanconi anemia pathway. *Blood* 2002; **100**: 4649–4654.
6 Guardiola P, Pasquini R, Dokal I, Ortega JJ, van Weel-Sipman M, Marsh JC *et al.* Outcome of 69 allogeneic stem cell transplantations for Fanconi anemia using HLA-matched unrelated donors: a study on behalf of the European Group for Blood and Marrow Transplantation. *Blood* 2000; **95**: 422–429.
7 Yabe H, Inoue H, Matsumoto M, Hamanoue S, Koike T, Ishiguro H *et al.* Allogeneic haematopoietic cell transplantation from alternative donors with a conditioning regimen of low-dose irradiation, fludarabine and cyclophosphamide in Fanconi anaemia. *Br J Haematol* 2006; **134**: 208–212.
8 MacMillan ML, Wagner JE. Haematopoeitic cell transplantation for Fanconi anaemia—when and how? *Br J Haematol* 2010; **149**: 14–21.
9 George B, Mathews V, Shaji RV, Srivastava V, Srivastava A, Chandy M. Fludarabine-based conditioning for allogeneic stem cell transplantation for multiply transfused patients with Fanconi's anemia. *Bone Marrow Transplant* 2005; **35**: 341–343.
10 Chaudhury S, Auerbach AD, Kernan NA, Small TN, Prockop SE, Scaradavou A *et al.* Fludarabine-based cytoreductive regimen and T-cell-depleted grafts from alternative donors for the treatment of high-risk patients with Fanconi anaemia. *Br J Haematol* 2008; **140**: 644–655.

nature
structural &
molecular biology

Formaldehyde catabolism is essential in cells deficient for the Fanconi anemia DNA-repair pathway

Ivan V Rosado[1], Frédéric Langevin[1], Gerry P Crossan[1], Minoru Takata[2] & Ketan J Patel[1,3]

Metabolism is predicted to generate formaldehyde, a toxic, simple, reactive aldehyde that can damage DNA. Here we report a synthetic lethal interaction in avian cells between *ADH5*, encoding the main formaldehyde-detoxifying enzyme, and the Fanconi anemia (FA) DNA-repair pathway. These results define a fundamental role for the combined action of formaldehyde catabolism and DNA cross-link repair in vertebrate cell survival.

Individuals afflicted with FA are prone to abnormal development and stem cell attrition and have a significant predisposition to cancer[1]. FA arises through germline inactivation of any one of 15 genes[2–4]. Most FA gene products operate together in an evolutionarily conserved pathway that eventually repairs DNA damage caused by certain chemotherapeutic agents that cross-link DNA[5–8]. However, such molecules cannot be the physiological source of DNA damage that precipitates the FA phenotype. Furthermore, chemotherapeutic cross-linkers cannot be the reason why the FA genes are conserved in all complex eukaryotes.

Recently we showed that acetaldehyde is a potential source of endogenous DNA damage necessitating repair by the FA-associated DNA-repair pathway[9]. However, acetaldehyde is not abundantly generated within cells, in contrast to formaldehyde (HCHO), the simplest reactive aldehyde[10]. Given that endogenous formaldehyde both is abundant and can attack DNA, we hypothesized that cells protect against this threat through the combined action of enzymatic detoxification and DNA repair. Here we examine the consequences of endogenous formaldehyde accumulation in DNA repair–deficient cell lines, revealing a fundamental role for the FA pathway in protecting cells against this reactive aldehyde.

Previous work has demonstrated that exogenous formaldehyde can be genotoxic. More specifically, chicken DNA repair–deficient cell lines deficient in the FA pathway downstream gene *FANCD2*, translesion synthesis (TLS) or homologous recombination (HR) show selective sensitivity to this aldehyde[11]. Formaldehyde-induced DNA damage has also been shown to be repaired by HR independently of the FA core complex[12]. We chose to extend these findings by testing formaldehyde genotoxicity in a human FA gene–deficient cell line (see **Supplementary Methods**). We used the human B cell line NALM-6 and its isogenic counterpart carrying an inactivation of the *FANCB* gene[13]. *FANCB*-deficient cells are very sensitive to formaldehyde (**Fig. 1a**),

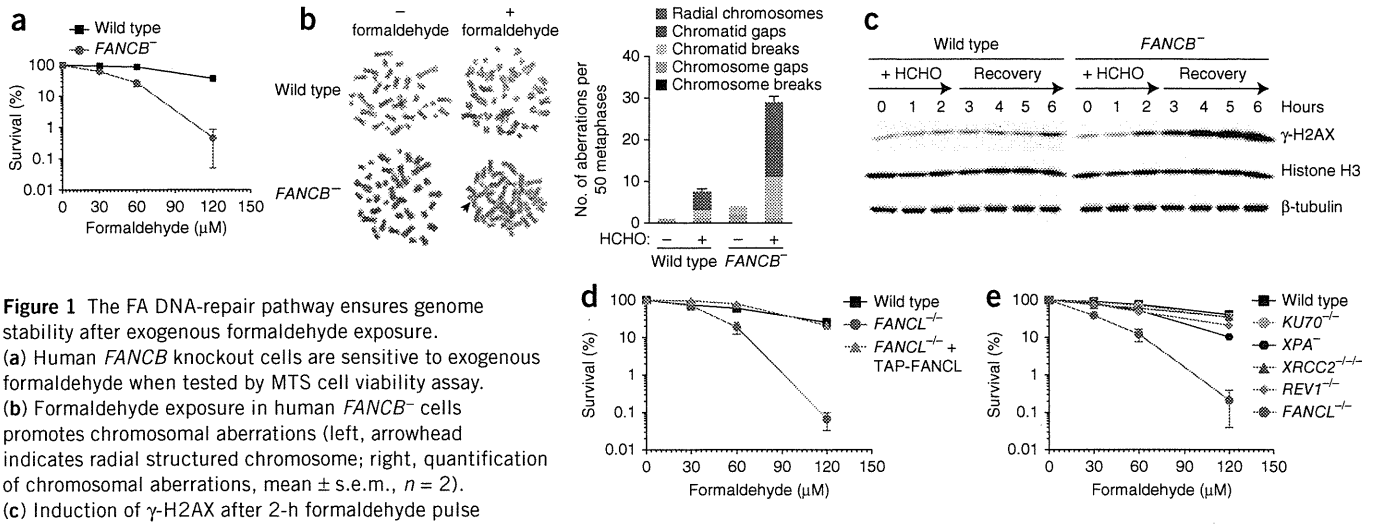

Figure 1 The FA DNA-repair pathway ensures genome stability after exogenous formaldehyde exposure. (**a**) Human *FANCB* knockout cells are sensitive to exogenous formaldehyde when tested by MTS cell viability assay. (**b**) Formaldehyde exposure in human *FANCB*⁻ cells promotes chromosomal aberrations (left, arrowhead indicates radial structured chromosome; right, quantification of chromosomal aberrations, mean ± s.e.m., $n = 2$). (**c**) Induction of γ-H2AX after 2-h formaldehyde pulse treatment and release. (**d**) *FANCL* DT40 knockout cells are hypersensitive to formaldehyde; *FANCL*-complemented cell line is resistant to formaldehyde. (**e**) DT40 knockouts *XRCC2*, *KU70* and *REV1* are not hypersensitive to formaldehyde; *XPA*-deficient cells are mildly sensitive to formaldehyde.

[1]Medical Research Council Laboratory of Molecular Biology, Cambridge, UK. [2]Laboratory of DNA Damage Signaling, Department of Late Effect Studies, Radiation Biology Center, Kyoto University, Kyoto, Japan. [3]University of Cambridge, Department of Medicine, Addenbrooke's Hospital, Cambridge, UK. Correspondence should be addressed to K.J.P. (kjp@mrc-lmb.cam.ac.uk).

Received 29 June; accepted 16 September; published online 13 November 2011; doi:10.1038/nsmb.2173

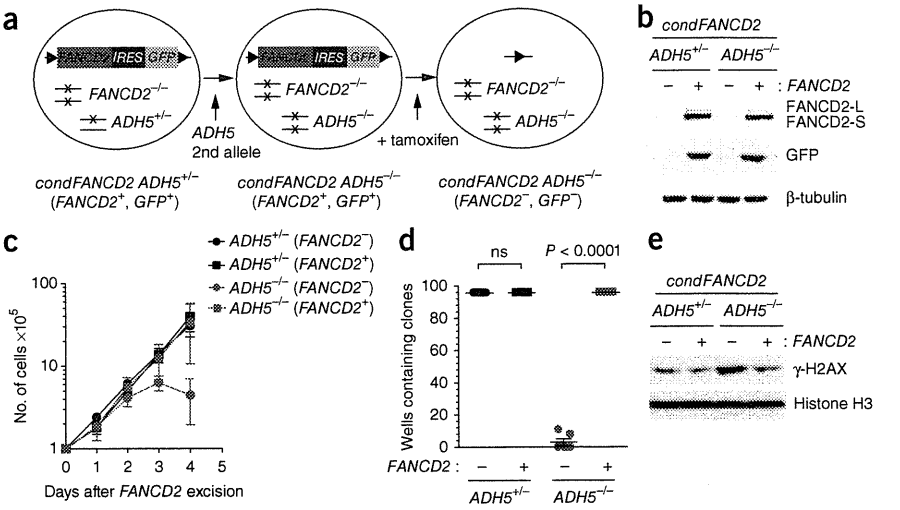

Figure 2 *FANCD2* and *ADH5* are synthetically lethal in DT40 cells. (**a**) Strategy outlining the conditional deletion of *FANCD2* in *ADH5*-null DT40 cells by addition of 4-OH tamoxifen. (**b**) Western blot of FACS GFP-positive (+) or -negative (–) sorted cells after 4-OH tamoxifen treatment for FANCD2 (top), GFP (middle) and β-tubulin (bottom). (**c**) Growth curve of FACS GFP$^+$ and GFP$^-$ sorted cells representing mean values of two independent experiments. Error bars define s.e.m. ($n = 2$). (**d**) Clonogenic survival assay of FACS GFP$^+$ and GFP$^-$ sorted cells plated at 50 cells per well into 96-well plates; mean values obtained from seven plates from two independent experiments. ($P < 0.0001$, Fisher's exact test. ns, nonsignificant.) (**e**) Induction of γ-H2AX in FACS GFP$^-$ and GFP$^+$ sorted cells lacking both *FANCD2* and *ADH5*.

and this sensitivity correlated with the accumulation of chromatid-type chromosome breakage and radial structure formation (**Fig. 1b**). These cells also showed enhanced induction of Ser139 phosphorylation of histone H2AX (γ-H2AX) (**Fig. 1c**), a marker of double strand breaks (DSBs).

We comprehensively tested formaldehyde sensitivity in both upstream and downstream components of the FA DNA-repair pathway using mutant chicken DT40 cell lines. Mutations in all the components of the FA pathway so far tested sensitized cells to formaldehyde (**Fig. 1d** and **Supplementary Fig. 1**). Cell lines deficient in the other major pathways of DNA repair were largely resistant to formaldehyde, with the exception of those deficient in nucleotide excision repair (specifically, mutant for the gene *XPA*), which showed mild sensitivity (**Fig. 1e**). In contrast to earlier results by others[11], we did not observe enhanced formaldehyde sensitivity in cells lines mutant for translesion synthesis (*REV1* and *REV3*) or homologous recombination (*XRCC2*, *XRCC3*, *RAD51C*, *RAD52* and *RAD54*) (**Supplementary Fig. 2**). This suggests that formaldehyde-induced DNA damage may not include interstrand cross-links.

Formaldehyde is generated endogenously within the nucleus as a byproduct of histone demethylation by the Jumonji demethylases and dealkylation of methylated DNA bases by AlkB orthologs (**Supplementary Fig. 3**)[10,14,15]. The cell prevents accumulation of endogenously generated formaldehyde through the action of alcohol dehydrogenase 5 (encoded by *ADH5*)[16]. To test whether the endogenous formaldehyde pool can be genotoxic, we generated an *ADH5*-knockout DT40 strain through gene disruption (**Supplementary Fig. 4a,b**). The *ADH5*$^{-/-}$ strain was readily obtained; this mutant's growth was not compromised, nor did it show increased sensitivity to exogenous formaldehyde under these conditions (**Supplementary Fig. 4c**). Next we attempted to inactivate the FA pathway in this strain by disruption of either the *FANCC* (one allele) or *FANCL* genes (two alleles). This proved unsuccessful (0/138 for *FANCC* and 0/781 for *FANCL*), suggesting that the combined inactivation of the FA pathway and *ADH5* could be synthetically lethal. We therefore constructed a DT40 *FANCD2*$^{-/-}$ strain that carries a conditional *FANCD2-IRES-GFP* expression cassette flanked by *lox*P sites (hitherto referred to as *condFANCD2*) (**Fig. 2a**). Owing to the presence of a 4-OH-tamoxifen–inducible Cre recombinase, 4-OH-tamoxifen treatment leads to excision of the *FANCD2-IRES-GFP* cassette, rendering the cells *FANCD2* deficient and *GFP* negative (*FANCD2*$^-$*GFP*$^-$). We then disrupted the *ADH5* gene in this strain to create the *condFANCD2 ADH5*$^{-/-}$ cell line, which lost FANCD2 and GFP expression upon treatment with 4-OH-tamoxifen, thereby generating *FANCD2*$^-$ *GFP*$^-$ cells. We purified this population by FACS (**Fig. 2b**) and followed the cells' fate in culture. The *FANCD2*$^-$ *GFP*$^-$ cells ceased growing after 3 d in culture (**Fig. 2c**), indicating that *FANCD2* has an essential role in cells lacking *ADH5*. Additionally, when *FANCD2*$^-$ *GFP*$^-$ cells were plated to isolate double-mutant clones, no viable *FANCD2*$^-$ *GFP*$^-$ cells were obtained in the *ADH5*$^{-/-}$ background (**Fig. 2d**). Finally, we observed a clear induction of γ-H2AX in the *FANCD2*$^-$ *GFP*$^-$ *ADH5*$^{-/-}$ cells but only a marginal increase in *FANCD2*$^-$ *GFP*$^-$ *ADH5*$^{+/-}$ cells (**Fig. 2e**).

In order to address whether the synthetically lethal interaction observed between *FANCD2* and *ADH5* was specific to the downstream component *FANCD2* or generalizable to core complex components, we generated a transcriptionally repressible *FANCL* knockout strain (**Fig. 3a**). The *ADH5*$^{+/-}$ cell was modified to express a *TAP-FANCL* transgene driven by a tetracycline-repressible promoter (*TetO*::*TAP-FANCL*). Both alleles of *FANCL* were knocked out in this strain, giving a *FANCL*$^{-/-}$*ADH5*$^{+/-}$ *TetO*::*TAP-FANCL* strain. We then proceeded to disrupt the second allele of *ADH5*, yielding the strain *FANCL*$^{-/-}$ *ADH5*$^{-/-}$ *TetO*::*TAP-FANCL*. Extinction of *TAP-FANCL* expression, and thus inactivation of the FA pathway, was observed upon addition of doxycycline to the culture medium. Within 2 d of doxycycline addition, TAP-FANCL expression was greatly diminished (**Fig. 3b**). This coincided with a cessation of proliferation and a marked decrease in viability only among cells deficient for *ADH5* (**Fig. 3c**). To quench endogenously produced formaldehyde, we exploited the chemistry between β-mercaptoethanol (β-ME) and aldehydes. Formaldehyde reacts readily with the thiol group of β-ME, giving a less reactive and more stable product, 2-((hydroxymethyl)thio) ethanol (**Supplementary Fig. 5**). Addition of 100 μM β-ME to the growth medium rescued the defect in cell proliferation and improved viability after repression of *TAP-FANCL* in *ADH5*$^{-/-}$ cells (**Fig. 3d**). Finally, using γ-H2AX as a marker of DSBs, we noted that cells lacking *ADH5* greatly induced γ-H2AX upon *FANCL* repression (**Fig. 3e**), in comparison to the *ADH5*-proficient cells. As predicted, addition of 100 μM β-ME suppressed this accumulation.

To summarize, we have shown by two independent approaches that inactivation of formaldehyde catabolism by disruption of *ADH5* results in synthetic lethality with upstream (*FANCL*) or downstream (*FANCD2*) components of the FA pathway. Our observation that FA-deficient chicken DT40 cells have an essential requirement for *ADH5* (and hence formaldehyde catabolism) contrasts with the requirement for *ALDH2* (encoding the enzyme that catabolizes acetaldehyde),

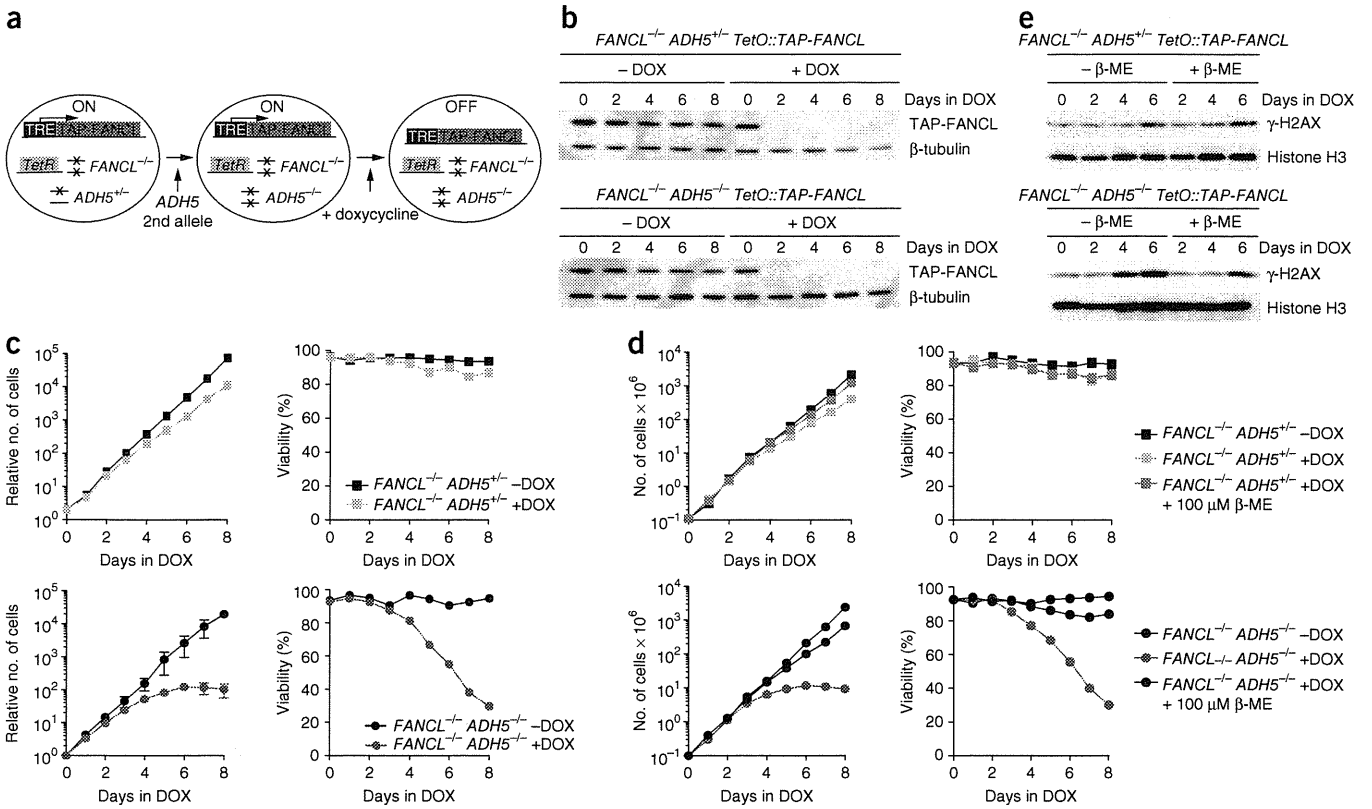

Figure 3 The FA core complex gene *FANCL* and *ADH5* are synthetically lethal in DT40 cells. (**a**) Strategy for conditional *FANCL* repression in *ADH5*-null DT40 cells by addition of doxycycline. (**b**) Conditional depletion of TAP-FANCL protein in doxycycline (DOX)-treated *FANCL*$^{-/-}$ *ADH5*$^{+/-}$ *TetO::TAP-FANCL* or *FANCL*$^{-/-}$ *ADH5*$^{-/-}$ *TetO::TAP-FANCL* cells. Whole cell extracts were western blotted with anti-tubulin IgG antibody (Sigma-Aldrich), which cross-reacts with TAP-FANCL. (**c**) Growth curves and viability plots of *FANCL* conditionally repressed cells in *ADH5*$^{+/-}$ and *ADH5*$^{-/-}$; each point represents mean values of two independent experiments. Error bars, s.e.m. (**d**) Growth curves of viable cells and viability plots of conditionally repressed *FANCL*$^{-/-}$ *ADH5*$^{+/-}$ or *ADH5*$^{-/-}$ *TetO::TAP-FANCL* cells in the presence of 2-mercaptoethanol (β-ME); each point represents mean values of two independent experiments. Error bars, s.e.m. (**e**) Induction of γ-H2AX following *FANCL* repression in *ADH5*$^{-/-}$ DT40 cells and its suppression following addition of β-ME.

whose absence is not synthetically lethal[9]. Thus, endogenous formaldehyde appears to be either more abundant and/or more potently genotoxic than acetaldehyde. It is striking that the full complement of FA genes is only found in higher eukaryotes; perhaps the expansion of FA genes coevolved with multicellularity and the emergence of stem cell pools[17,18]. Because we know that formaldehyde is produced as a byproduct of histone demethylation, our results lead us to predict that certain cell lineages with a propensity for extensive histone modifications might be particularly reliant on FA pathway repair. Endogenous formaldehyde genotoxicity might therefore explain the progressive attrition of germ and blood stem cells in FA.

Note: Supplementary information is available on the Nature Structural & Molecular Biology website.

ACKNOWLEDGMENTS

We thank N. Adachi and H. Koyama (Kihara Institute for Biological Research, Japan) for kindly providing NALM-6 human cell lines. We are grateful to J. Sutherland and K. Lang (MRC Laboratory of Molecular Biology) for chemical insight and to M. Daly and F. Zhang (MRC Laboratory of Molecular Biology) for invaluable help with flow cytometry. I.V.R. and F.L. are funded by the Fanconi Anaemia Research Fund and Children's Leukaemia Trust, respectively.

AUTHOR CONTRIBUTIONS

I.V.R. and K.J.P. designed the study and the experiments, and wrote the paper. I.V.R. performed the majority of the experiments presented. F.L. contributed to DT40 clonogenic assays and assisted in the generation of *ADH5*-deficient cell lines. G.P.C. helped with analysis of chromosome breaks. M.T. generated and provided the FANCD2 inducible cell line.

COMPETING FINANCIAL INTERESTS

The authors declare no competing financial interests.

Published online at http://www.nature.com/nsmb/.
Reprints and permissions information is available online at http://www.nature.com/reprints/index.html.

1. Muller, L.U. & Williams, D.A. *Mutat. Res.* **668**, 141–149 (2009).
2. Crossan, G.P. *et al. Nat. Genet.* **43**, 147–152 (2011).
3. Stoepker, C. *et al. Nat. Genet.* **43**, 138–141 (2011).
4. Kim, Y. *et al. Nat. Genet.* **43**, 142–146 (2011).
5. Joenje, H. & Patel, K.J. *Nat. Rev. Genet.* **2**, 446–457 (2001).
6. Patel, K.J. & Joenje, H. *DNA Repair (Amst.)* **6**, 885–890 (2007).
7. de Winter, J.P. & Joenje, H. *Mutat. Res.* **668**, 11–19 (2009).
8. Rosado, I.V., Niedzwiedz, W., Alpi, A.F. & Patel, K.J. *Nucleic Acids Res.* **37**, 4360–4370 (2009).
9. Langevin, F., Crossan, G.P., Rosado, I.V., Arends, M.J. & Patel, K.J. *Nature* **475**, 53–58 (2011).
10. Mosammaparast, N. & Shi, Y. *Annu. Rev. Biochem.* **79**, 155–179 (2010).
11. Ridpath, J.R. *et al. Cancer Res.* **67**, 11117–11122 (2007).
12. Noda, T. *et al. Biochem. Biophys. Res. Commun.* **404**, 206–210 (2011).
13. Nomura, Y., Adachi, N. & Koyama, H. *Genes Cells* **12**, 1111–1122 (2007).
14. Trewick, S.C., Henshaw, T.F., Hausinger, R.P., Lindahl, T. & Sedgwick, B. *Nature* **419**, 174–178 (2002).
15. Falnes, P.O., Johansen, R.F. & Seeberg, E. *Nature* **419**, 178–182 (2002).
16. Iborra, F.J. *et al. J. Histochem. Cytochem.* **40**, 1865–1878 (1992).
17. Mosedale, G. *et al. Nat. Struct. Mol. Biol.* **12**, 763–771 (2005).
18. Zhang, X.Y. *et al. PLoS Genet.* **5**, e1000645 (2009).

Int J Hematol (2011) 93:415–416
DOI 10.1007/s12185-011-0832-9

Guest editorial: fanconi anemia and the DNA damage response

Minoru Takata

Received: 2 March 2011 / Revised: 8 March 2011 / Accepted: 22 March 2011 / Published online: 12 April 2011

Every cell in our body other than red blood cells has a genome, the stability of which is crucial for life. The DNA is precisely replicated during cell proliferation, and is stably maintained, even after terminal differentiation, as a repository of information that orchestrates the cell's metabolism. Unfortunately, our world is full of potential threats to genomic stability. DNA may degrade spontaneously, errors may occur during its replication, or metabolic byproducts, such as oxygen radicals or aldehydes, may chemically modify its nucleotide bases (i.e. DNA adducts). Ionizing radiation, ultraviolet light, and chemotherapeutic drugs are all well-known exogenous sources of DNA damage [1, 2].

To ensure cellular fitness, organisms have developed an elaborate molecular network to detect and repair DNA damage [3]. If deleterious effects of DNA damage exceed the cell's repair capacity, it accumulates in the genome, leading to activation of cell cycle checkpoints (buying time for repair), cell death (apoptosis or necrosis), or, in the failure of checkpoints or cell death, conversion of DNA damage to mutations. This may result in poor cell proliferation, emergence of malignancy, impaired stem cell maintenance, or early-onset aging [1, 2]. Since all cellular activity in a way relies on the genome, the mechanisms that govern genomic stability are fundamentally important in biomedical research in general. Blood cells are no exception.

As our knowledge of genomic stability has expanded massively in recent years, a rare hematological disorder, Fanconi anemia (FA), has become a prototypical example among hereditary conditions involving a defect in the DNA damage response (DDR). FA is one of several disorders discovered by the prominent Swiss pediatrician Guido Fanconi [4]. His first report in 1927 described brothers presenting with a pernicious anemia-like condition, congenital anomalies, and hyper-pigmentation of the skin. In the 1960s and 70s, it was established that FA cells display chromosomal instability, which is particularly pronounced following treatment with mitomycin C [5, 6]. The first molecular cloning of an FA gene was achieved by functional complementation using a cDNA expression library in the early 1990s [7]. However, until quite recently, the true molecular defect in FA, which is now considered to affect the response to replication stress, had not been defined.

There seem to be a number of reasons why FA attracts widespread attention today. First of these is that novel FA genes continue to be identified year after year. This trend began at the turn of the 21st century, and has continued into this year, with the current number of the FA genes now totaling 15 [8–10]. This is surprising. Second, FA patients with disparate mutations display essentially similar phenotypes, strongly suggesting the presence of a common signal transduction pathway consisting of the FA gene products (i.e. FA pathway) [11, 12]. This prediction was well confirmed by the identification of the FA core complex (i.e. interactions between the FA core components FANCA/B/C/E/F/G/M/L) as an E3 ubiquitin ligase, and DNA damage-induced monoubiquitination of FANCD2 and FANCI, which is absent in cells lacking the core complex members [11, 12]. Of note, posttranslational protein modifications, such as ubiquitination, are currently the focus of intensive research in this field [13, 14]. Third, the discovery that the FANCD1 gene is the breast cancer

M. Takata (✉)
Laboratory of DNA Damage Signaling,
Department of Late Effect Studies,
Radiation Biology Center, Kyoto University, Kyoto, Japan
e-mail: mtakata@house.rbc.kyoto-u.ac.jp

suppressor BRCA2 has had an enormous impact [15]. This means that the FA pathway has a strong connection with the much more common disease, familial breast cancer. Fourth, hematopoietic stem cells are affected in FA. Thus, it is perhaps not unexpected that FA is one of the first disorders for which patient-derived induced pluripotent stem (iPS) cells have been generated [16]. In addition to the above, there are numerous other very interesting studies of FA that I cannot mention here.

To provide some perspective on FA and the DNA damage response, this issue of IJH publishes a set of review articles as part of the "Progress of Hematology" series. In addition to our own account of FA, this collection contains up-to-date summaries regarding the maintenance of hematopoietic stem cells and the DNA damage response, the exciting discovery of the BLM helicase-FA relationship in ultrafine chromosomal bridges, and the molecular mechanisms, such as ubiquitination, that are activated in response to DNA double strand breaks, and their dysfunction in primary immunodeficiency syndromes. I trust our readers will find these reviews to be interesting, and useful in their work.

References

1. Hoeijmakers JH. Genome maintenance mechanisms for preventing cancer. Nature. 2001;411:366–74.
2. Rouse J, Jackson SP. Interfaces between the detection, signaling, and repair of DNA damage. Science. 2002;297:547–51.
3. Harper JW, Elledge SJ. The DNA damage response: ten years after. Mol Cell. 2007;28:739–45.
4. Lobitz S, Velleuer E. Guido Fanconi (1892–1979): a jack of all trades. Nat Rev Cancer. 2006;6:893–8.
5. Sasaki MS, Tonomura A. A high susceptibility of Fanconi's anemia to chromosome breakage by DNA cross-linking agents. Cancer Res. 1973;33:1829–36.
6. Sasaki MS. Is Fanconi's anaemia defective in a process essential to the repair of DNA cross links? Nature. 1975;257:501–3.
7. Strathdee CA, Gavish H, Shannon WR, Buchwald M. Cloning of cDNAs for Fanconi's anaemia by functional complementation. Nature. 1992;356:763–7.
8. Crossan GP, van der Weyden L, Rosado IV, et al. Disruption of mouse Slx4, a regulator of structure-specific nucleases, phenocopies Fanconi anemia. Nat Genet. 2011;43:147–52.
9. Kim Y, Lach FP, Desetty R, Hanenberg H, Auerbach AD, Smogorzewska A. Mutations of the SLX4 gene in Fanconi anemia. Nat Genet. 2011;43:142–6.
10. Stoepker C, Hain K, Schuster B, et al. SLX4, a coordinator of structure-specific endonucleases, is mutated in a new Fanconi anemia subtype. Nat Genet. 2011;43:138–41.
11. Wang W. Emergence of a DNA-damage response network consisting of Fanconi anaemia and BRCA proteins. Nat Rev Genet. 2007;8:735–48.
12. Kee Y, D'Andrea AD. Expanded roles of the Fanconi anemia pathway in preserving genomic stability. Genes Dev. 2010; 24:1680–94.
13. Cohn MA, D'Andrea AD. Chromatin recruitment of DNA repair proteins: lessons from the fanconi anemia and double-strand break repair pathways. Mol Cell. 2008;32:306–12.
14. Huang TT, D'Andrea AD. Regulation of DNA repair by ubiquitylation. Nat Rev Mol Cell Biol. 2006;7:323–34.
15. Howlett NG, Taniguchi T, Olson S, et al. Biallelic inactivation of BRCA2 in Fanconi anemia. Science. 2002;297:606–9.
16. Raya A, Rodriguez-Piza I, Guenechea G, et al. Disease-corrected haematopoietic progenitors from Fanconi anaemia induced pluripotent stem cells. Nature. 2009;460:53–9.

Japanese Journal of Transfusion and Cell Therapy, Vol. 58. No. 1 58(1) : ***—***, 2012

—[Original]— 原 著—

PYRUVATE SUPPLEMENTATION ENHANCES VASCULAR ENDOTHELIAL GROWTH FACTOR PRODUCTION BY BONE MARROW-DERIVED MONONUCLEAR CELLS

Hitoshi Kanno[1)2)], *Yuji Iribe*[1)], *Takako Aoki*[2)], *Hiromi Ogura*[1)] *and Hisaichi Fujii*[1)]

Bone marrow-derived mononuclear cells (BMMNC) include endothelial progenitor cells (EPC), which are characterized by their secretion of angiogenic factors such as vascular endothelial growth factor (VEGF) to recruit local endothelial cells, thereby enabling the establishment of new blood vessels. Implantation of BMMNC has been clinically used for therapeutic purposes in the treatment of critical limb ischemia (CLI); results showed that it was ineffective in a substantial number of cases. To evaluate the appropriate concentration of pyruvate to achieve the highest VEGF gene expression, cells were cultured with pyruvate at final concentrations up to 20 mM in 5% CO_2 for 2-4 days. The intracellular concentration of pyruvate was measured enzymatically and cell number and viability were determined. Expression levels of VEGF genes and numbers of $CD31^+/CD34^+$ cells were evaluated. Finally, VEGF levels in the conditioned medium were examined in each condition. Pyruvate supplementation in murine BMMNC cultures successfully increased intracellular pyruvate levels in a concentration-dependent manner, and 5 mM pyruvate was found to be the most appropriate to maintain viable cell number and up-regulate *VEGF* gene after 2-day culture. In addition, VEGF in the conditioned medium was significantly elevated by the use of 5 mM pyruvate after 4-day culture. From these results, we suggest that preconditioning of BMMNC with 5 mM pyruvate for 2 days may be a useful way to safely and inexpensively enhance the angiogenic properties of BMMNC and the therapeutic effectiveness of cellular therapy for CLI.

Keywords: critical limb ischemia, regenerative medicine, vascular endothelial growth factor, Endothelial progenitor cells

INTRODUCTION

Critical limb ischemia (CLI) is the end-stage status of arterial stenosis or obstruction in the lower extremities due to arteriosclerotic peripheral artery disease (PAD) or thromboangitis obliterans (TAO, Buerger's disease). CLI is characterized by symptoms such as leg pain, skin ulcers or uncontrollable infection, eventually resulting in limb amputation due to necrosis of the affected leg. For patients suffering from severely ischemic legs, surgical bypass grafting or endoatherectomy has been applied; however, approximately 20-30% of patients are not candidates for these procedures. As a result, about 100,000 and 120,000 CLI patients undergo leg amputation per year in the European Union and United States, respectively[1)].

Bone marrow-derived mononuclear cells (BMMNC) have been demonstrated to contain endothelial progenitor cells (EPC), which secrete angiogenic factors and recruit endothelial colony-forming cells with proliferative potential for neoangiogenesis[2)–5)]. Implantation of BMMNC or peripheral blood mononuclear cells (PBMNC) has been used for therapeutic neovascularization and is becoming an indispensable therapeutic option to rescue ischemic limbs. In Japan, the clinical feasibility of this approach has been analyzed in a randomized controlled study called TACT: Therapeutic Angiogenesis by Cell Transplantation[6)]. Three-year amputation-free rates were 91% in TAO and 60% in PAD, suggesting that cellular therapy is effective for most patients affected by TAO, but that several obstacles must be overcome to improve overall clinical effectiveness, especially for PAD. A Phase I/IIa clinical trial

1) Department of Transfusion Medicine and Cell Processing, Tokyo Women's Medical University
2) Institute of Medical Genetics, Tokyo Women's Medical University

[Received: **/*/*, Accepted: **/*/*]
2011/8/16 2011/12/23

reported that granulocyte-colony stimulating factor (G-CSF)-mobilized $CD34^+$ cells were safely utilized and that improvement of efficacy was revealed both subjectively and objectively[7].

Normal cells can activate genes in the adaptation to a hypoxic environment, and hypoxia-inducible factor (HIF-1) is known to be responsible for transcriptional activation. HIF-1 acts as a heterodimer, and a subunit, HIF-1α, becomes unstable in normoxic conditions. An exception to this is in cancer cells, where it is stable under normoxic conditions[8]. Subsequently, hypoxia-inducible genes such as glucose transporters, glycolytic enzymes, erythropoietin, carriers for iron/copper, and vascular endothelial growth factor (VEGF) and its cognate receptor are activated, leading to neoangiogenesis accompanying tumor formation.

HIF-1α is post-translationally regulated by two oxygen sensors, HIF prolylhydroxylase (HIF-PH) and FIH (factor-inhibiting HIF). Under normoxia, HIF-PH hydroxylates both $proline^{402}$ and $proline^{564}$, resulting in degradation by the ubiquitin-proteasome pathway. Similarly, FIH hydroxylates $aspargine^{803}$, and this hydroxylation interferes with the protein-protein interaction between HIF and CBP/p300[9]. 2-oxoglutarate is a crucial cofactor for HIF-PH and pyruvate binds to the 2-oxoglutarate site of HIF-PH, leading to stabilization of HIF-1 through inactivation of HIF-PH[10]. As a result, pyruvate enables HIF-mediated trans-activation of genes associated with the mobilization, migration and recruitment of endothelial cells to form new blood vessels.

VEGF is an angiogenic growth factor which is activated through HIF-1α stabilization. Previous studies attempted to enhance VEGF production of EPC using hypoxic preconditioning[11] or HIF-PH inhibitors[12]. In the present study, we show that preconditioning of BMMNC using an appropriate concentration of pyruvate successfully activates *VEGF* gene and augments VEGF production, and discuss the possible application of short-period conditioning to cellular therapy for CLI.

MATERIALS AND METHODS

Tissues and cells

Male C57BL/6 mice aged 7-8 weeks were obtained from Japan SLC (Shizuoka, Japan) and housed under pathogen-free conditions. Bone marrow cells were obtained from femurs and tibiae aseptically by flushing with RPMI1640 into 15-m*l* plastic tubes using a 21-gauge needle and a 1-m*l* syringe. Clumps of cells were dispersed by repeated passage through the 21-gauge needle. The bone marrow cells were the washed with RPMI1640 once, and mononuclear cells were obtained after Ficoll-Paque density gradient centrifugation. Aliquots of bone marrow cells were diluted in Turk's solution and nucleated cells were counted. Cells were maintained in RPMI1640 medium (Invitrogen, Carlsbad, CA) supplemented with 10% heat-inactivated fetal calf serum (FCS), and a mixture of penicillin-streptomycin (Sigma-Aldrich, St. Louis, MO).

Measurement of intracellular concentration of pyruvate

To evaluate the effects of pyruvate on hypoxia-inducible gene expression, BMMNC (8e5 cells/m*l*) were cultured in RPMI1640 supplemented with 10% FCS and pyruvate at final concentrations of 0, 1, 3, 5, 10 and 20 mM in 5% CO_2 at 37℃ for 2-4 days. Viability was calculated by the trypan blue dye exclusion method. A murine leukemic cell line, CBA2, was used as a control[13].

Cultured cells were collected by centrifugation at 800 g, 4℃, for 3 minutes, and washed with ice-cold PBS once. The cell pellet was resuspended with 2 m*l* of 0.3 N perchloride, and rigorously mixed by vortexing. After centrifugation at 5,000 g, 4℃, for 5 minutes, supernatants were used to measure the intracellular concentration of pyruvate as previously described[14]. Protein assays were performed by the method of Bradford using a commercial kit (Bio-Rad Protein Assay Kit, Bio-Rad Laboratories, Hercules, CA).

We purchased cobalt chloride, L-mimosine and roscovitin from Sigma (USA). These reagents were used as HIF-PH inhibitors, and final concentrations in culture medium were 75 μM, 1 mM and 20 μM, respectively.

Flow cytometric analysis

Fluorescence-activated cell sorting (FACS) analysis was performed using the EPICS ALTRA analyzer XL-MCL (Beckman Coulter, USA), and the data were analyzed with EXPO™32 ADC software (Beckman Coulter, USA). Antibodies against human CD31 and CD34 labeled with FITC (fluorescein isothiocyanate) and PE (phycoerythrin), respectively, were obtained from Beckman Coulter.

Quantitative RT-PCR (Q-RTPCR)

Total cellular RNA of cultured BMMNC was extracted with an RNeasy purification kit (QIAGEN), and

Table 1 Oligonucleotide primers used in this study

VEGF-1	5'-GAGCTTCCTACAGCACAGCA-3'
VEGF-2	5'-TCTTTCCGGTGAGAGGTCTG-3'
GAPD-1	5'-TGCGACTTCAACAGCAACTC -3'
GAPD-2	5'-ATTGTGAGGGAGATGCTCAG-3'

500 ng of total RNA was reverse-transcribed at 42℃ for 90 minutes with 50 pmol oligo (dT) 17 primer, 0.5 U/μl cloned RNase inhibitor (Takara Bio, Shiga, Japan), 10 mM DTT, 1 mM dNTP and 50 units of Expand Reverse Transcriptase (Roche Diagnostics). Aliquots (1/100) were subjected to quantitative reverse-transcription PCR (Q-RTPCR) using primer pairs described in Table 1. Q-RTPCR was performed using Mx3000P (Stratagene, CA) with SYBR Premix ExTaq polymerase (Takara Bio). The reaction mixtures were subjected to 40 cycles of amplification consisting of 95℃ for 30 seconds, 63℃ for 60 seconds and 72℃ for 30 seconds. Primers are listed in Table 1.

Relative gene expression levels were calculated using the standard curve, which was made by Q-RTPCR using 0, 0.8, 4, 20 and 100 ng of total RNA extracted from untreated murine BMMNC. The glyceraldehyde-3-phosphate dehydrogenase (*GAPDH*) mRNA level was used as an internal control.

Measurement of VEGF excretion

After 4-day culture, conditioned medium was used to determine VEGF concentration using the Quantikine-Mouse VEGF Immunoassay (R&D Systems, USA). VEGF concentration is expressed as picograms per milliliter of conditioned medium, and calculated mean and standard error (SE) of three independent experiments were used for statistical analysis. Statistical comparisons between groups were performed using Student's t test. $P<0.05$ was considered statistically significant.

RESULTS

In order to evaluate whether BMMNC can efficiently uptake extracellular pyruvate in culture medium, we measured the intracellular concentration of pyruvate after 2-day culture. As shown in Fig. 1, supplementation of pyruvate resulted in accumulation of intracellular pyruvate in a concentration-dependent manner. Using 20 mM pyruvate, accumulation was increased 33-fold. In contrast, we were unable to observe the accumulation of intracellular pyruvate with a leukemic cell line (data not shown).

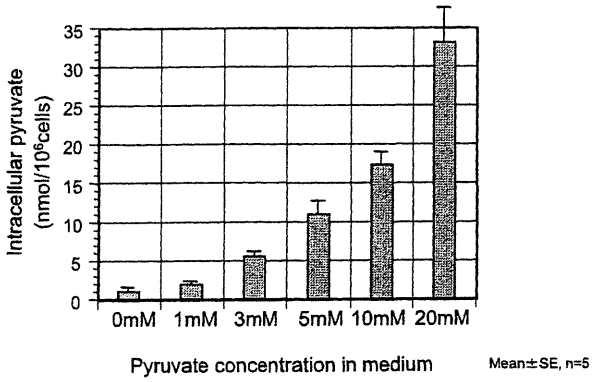

Fig. 1 Intracellular pyruvate concentration after a short period of culture supplemented with pyruvate. Supplementation of pyruvate for 2 days resulted in accumulation of intracellular pyruvate in a concentration-dependent manner. Intracellular pyruvate concentrations were as follows: 0 mM, 1.11±0.51; 1 mM, 2.00±0.37; 3 mM, 5.61±0.57; 5 mM, 11.04±1.66; 10 mM, 17.39±1.59; 20 mM, 33.15±4.50 (n=5, mean±SE).

Fig. 2 depicts numbers of viable BMMNC after 2- or 4-day culture with various concentrations of pyruvate added to the culture medium. Cell number on day 0 was designated as 1. On day 2, 5 mM pyruvate most significantly increased the viable cell number compared with the others (paired t-test, two-tailed p-value< 0.01, n=3), to approximately two-fold that on day 0. In contrast, cell number on day 4 was decreased to less than half of that on day 2, and no significant differences were recognized between 3, 5 and 10 mM pyruvate.

Flow cytometry was used to evaluate circulating EPC level by the quantification of cells double-positive for EPC markers defined as $CD31^+/CD34^+$. A representative scatter graph is shown in Fig. 3. Although no statistical analysis was carried out, 5 mM pyruvate for 4 days seemed more effective for the increment of $CD31^+/CD34^+$ cells.

Next, we further studied the influence of other HIF-PH inhibitors, such as cobalt chloride, L-mimosine and roscovitin, on the induction of VEGF. After 2-day culture of BMMNC supplemented with 0, 1, 3 and 5 mM pyruvate, or other HIF-PH inhibitors, VEGF mRNA was measured by Q-RTPCR (Fig. 4). *VEGF* mRNA quantities included in 5 ng of RNA from each condition are shown with untreated murine BMNC as a control. Supplementation with 1, 3 and 5 mM pyruvate augmented *VEGF* mRNA up to approximately 8.4, 20.9 and 27.8 times, respectively. Among the HIF-PH inhibi-

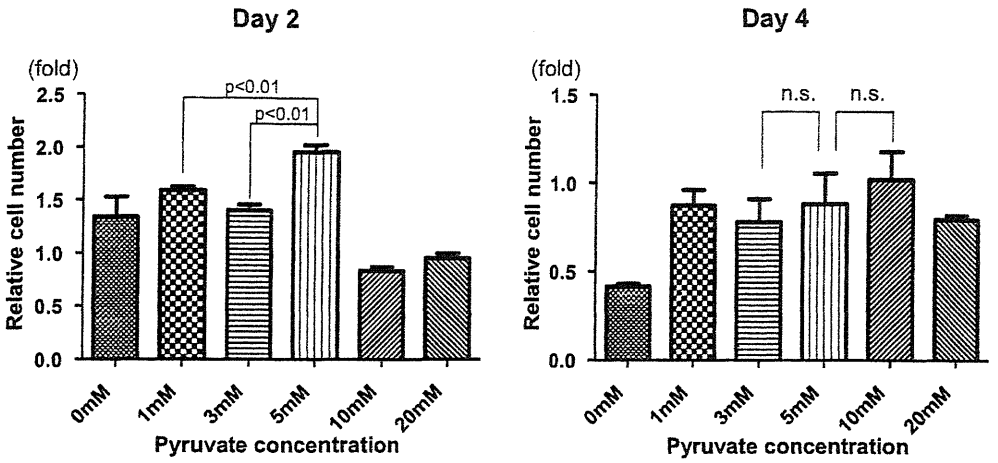

Fig. 2 Cell proliferation and viability after a short period of culture supplemented with pyruvate. Viable cell numbers after 2- or 4-day culture with various concentrations of pyruvate in culture medium are shown. On day 2, 5 mM pyruvate most significantly increased the viable cell number (1.96-fold) compared with 1 mM (1.59-fold), 3 mM (1.40-fold) and others (paired t-test, two-tailed p value$<$0.01. n = 3). On day 4, no significant differences were recognized between 3, 5 and 10 mM pyruvate.

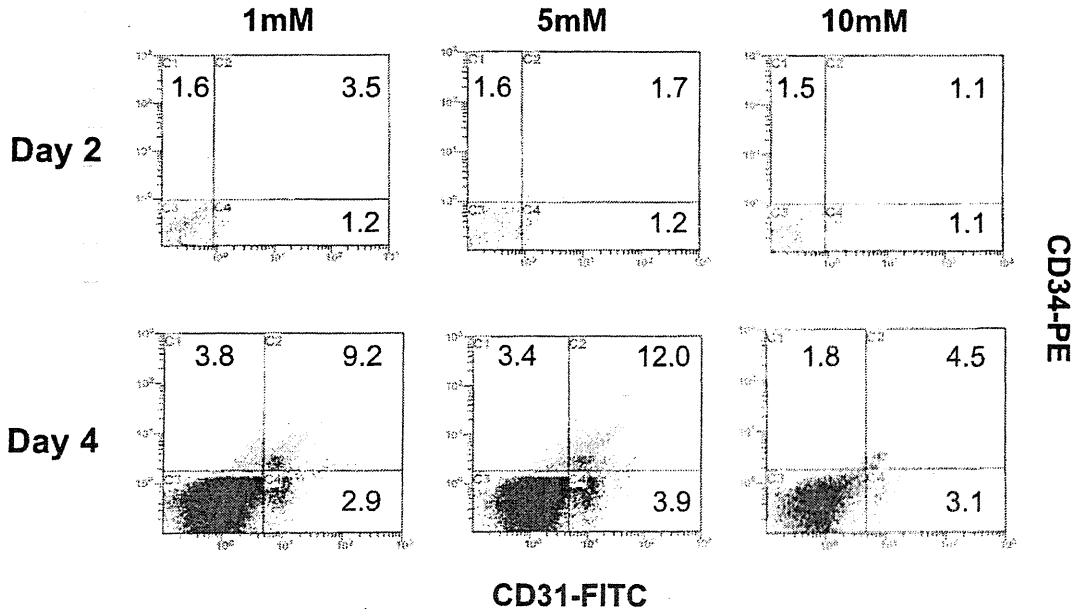

Fig. 3 $CD31^+/CD34^+$ cells after 4-day culture with various concentrations of pyruvate
As $CD31^+/CD34^+$ cell fraction contains EPC, we evaluated these cell surface markers by flow cytometry. Untreated BMMNC contain 1.0%, 4.3% and 1.6% of $CD31^+/CD34^-$, $CD34^-/CD34^+$ and $CD31^+/CD34^+$ cells, respectively (data not shown). Numbers in scatter graphs indicate % of the corresponding fractions. No obvious increment of $CD31^+/CD34^+$ cells was observed on day 2, while 4-day culture resulted in an increase in double-positive cells to 9.2% at 1 mM, 12.0% at 5 mM, and 4.5% at 10 mM.

tors tested, cobalt chloride showed the largest increase in *VEGF* mRNA, at approximately 109 times more than the control. Levels with L-mimosine and roscovitine were 28.3 and 42.1 times more than that of the control, respectively.

Finally, we examined VEGF concentration in conditioned medium (Fig. 5). In this experiment, only the 4-day culture with 5 mM pyruvate showed significant elevation of excreted VEGF level compared with 0 mM pyruvate (n=5, two-tailed p value$<$0.05).

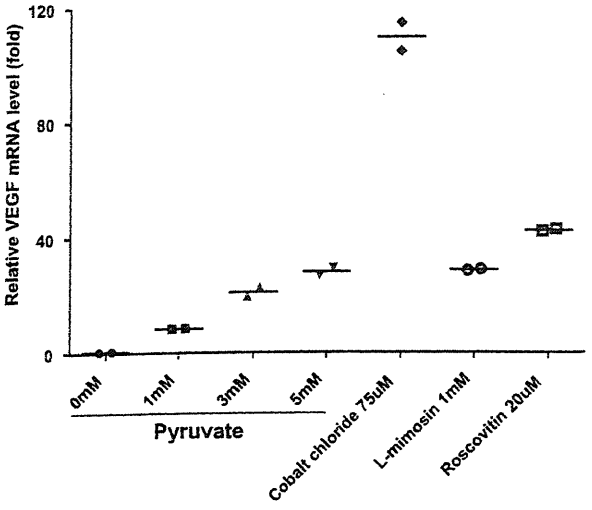

Fig. 4 Transcriptional activation of VEGF gene by pyruvate compared with activation by other HIF-PH inhibitors.
VEGF mRNA was titrated after 2-day treatment with pyruvate as well as other HIF-PH inhibitors. Vertical axis shows relative *VEGF* mRNA quantities compared with those of untreated murine BMMNC as a control. Data of two independent experiments are shown. *VEGF* mRNA increased 8.4 times at 1 mM, 20.9 times at 3 mM and 27.8 times at 5 mM, compared with that of untreated murine BMMNC. Levels with HIF-PH inhibitors such as cobalt chloride, L-mimosine and roscovitine were 109, 28.3 and 42.1 times more than control, respectively.

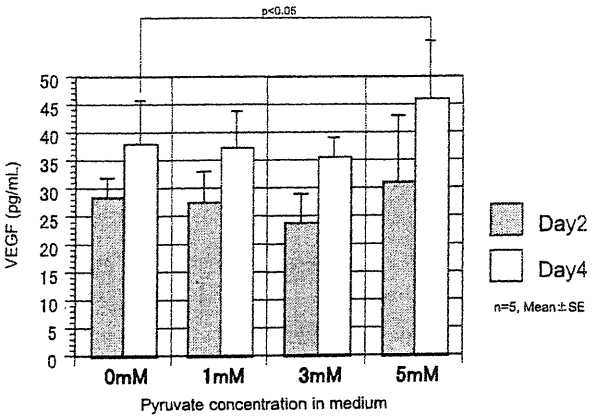

Fig. 5 VEGF levels in the conditioned medium
VEGF concentration in the medium was measured after 2- and 4-day culture, and statistical analysis was performed by paired t-test ($n=5$). A significant increase was observed only for 5 mM pyruvate on day 4 (two-tailed p value <0.05).

DISCUSSION

EPC can be recruited from bone marrow by several growth factors, such as VEGF, stromal cell-derived factor-1 (SDF-1), angiopoietin-1 or G-CSF[15]. EPC also secretes VEGF in autocrine and paracrine fashions, and acts to differentiate mature EPC into endothelial cells[16]. Thus, activation of *VEGF* gene in EPC is most likely to be effective in augmenting therapeutic efficacy for CLI patients. Previous studies have elucidated that circulating EPC express several endothelial cell-specific surface markers such as CD31, CD34, VEGF receptor-2, CD146 and von Willebrand factor[17].

In order to examine whether BMMNC can efficiently uptake extracellular pyruvate in a short-period culture, we measured the intracellular concentration of pyruvate after 2- and 4-day culture. As shown in Fig. 1, the intracellular concentration of pyruvate successfully increased in an extracellular pyruvate concentration-dependent manner. Carry-over of extracellular pyruvate in assay samples was unlikely, since intracellular pyruvate was unchanged in a leukemic cell line, which rapidly proliferates in culture. Viable cell counts were evaluated using 1-20 mM pyruvate in medium (Fig. 2), and 5 mM pyruvate was shown to be the most appropriate concentration to increase viable cells on day 2, whereas no significant differences were observed among 1-10 mM pyruvate on day 4. Numbers of $CD31^+/CD34^+$ double-positive cells were increased in 5 mM pyruvate on day 4 (Fig. 3), and 5 mM pyruvate upregulated *VEGF* gene to the same extent as L-mimosine on day 2 (Fig. 4). It should be noted that VEGF concentration in conditioned medium showed a significant increase at 5 mM on 4-day culture. Since viable cell numbers and *VEGF* mRNA became significantly enhanced on day 2, and secreted VEGF in conditioned medium must be washed out and resuspended in saline before administration, we conclude that 2-day culture in 5 mM pyruvate is the most appropriate condition for enhancing VEGF production of murine BMMNC.

Mechanisms attributable to the activation of HIF-inducible genes under normoxia have been extensively studied, and several chemicals and organic small molecules have been identified as HIF-PH inhibitors[12]. Roscovitine is a purine derivative, and inhibits cyclin-dependent kinase, inducing cell cycle arrest and apoptosis. This chemical is under consideration as a potential anti-tumor reagent. L-mimosine is a plant amino acid that has a similar structure to tyrosine, and also induces cell cycle arrest in mammalian cells and inhibits translation of cyclin-dependent kinase. Cobalt chloride and roscovitin showed greater effectiveness for *VEGF*

gene activation (Fig. 4); however, both are much more expensive and have cytotoxicity, which is a serious concern when cells are administered to patients.

Although a previous report demonstrated that pyruvate is effective for angiogenesis in chick embryo[18] as well as in *in vivo* mouse Matrigel plug assays, we confirmed that pyruvate supplementation raised the intracellular concentration in culture and that VEGF concentration was increased in conditioned medium. *Ex vivo* activation of the hypoxia-inducible genes and subsequent administration of cells are considered to not only enhance clinical effectiveness but to also provide a novel approach in cellular therapy for CLI, since a recent study[19] showed that the conditioned medium generated from *in vitro* culture of progenitor cells was effective for CLI.

Quite recently, a prospective, randomized, double-blinded clinical study revealed a significant increase in amputation-free survival in patients receiving cellular therapy for CLI[20]. In the study, autologous bone marrow cells were used, designated as tissue repair cells (TRC), which were generated by 12-day culture in long-term bone marrow culture medium[21]. TRC are derived from a 50-m*l* bone marrow aspirate, and reportedly contained more $CD14^+$ and $CD90^+$ cells than primary BMMNC[21].

In conclusion, the present study showed that this culture system successfully enhanced *VEGF* gene expression and secretion of VEGF into the medium. *Ex vivo* expansion of EPC may become an ideal strategy as a cellular source for therapeutic neoangiogenesis.

References

1) Lawall H, Bramlage P, Amann B: Stem cell and progenitor cell therapy in peripheral artery disease. A critical appraisal. Thromb Haemost, 103: 696—709, 2010.
2) Kinnaird T, Stabile E, Burnett MS, et al: Local delivery of marrow-derived stromal cells augments collateral perfusion through paracrine mechanisms. Circulation, 109: 1543—1549, 2004.
3) Ziegelhoeffer T, Fernandez B, Kostin S, et al: Bone marrow-derived cells do not incorporate into the adult growing vasculature. Circ Res, 94: 230—238, 2004.
4) Rehman J, Li J, Orschell CM, et al: Peripheral blood "endothelial progenitor cells" are derived from monocyte/macrophages and secrete angiogenic growth factors. Circulation, 107: 1164—1169, 2003.
5) Tateno K, Minamino T, Toko H, et al: Critical roles of muscle-secreted angiogenic factors in therapeutic neovascularization. Circ Res, 98: 1194—1202, 2006.
6) Matoba S, Tatsumi T, Murohara T, et al: Long-term clinical outcome after intramuscular implantation of bone marrow mononuclear cells (Therapeutic Angiogenesis by Cell Transplantation [TACT] trial) in patients with chronic limb ischemia. Am Heart J, 156: 1010—1018, 2008.
7) Kawamoto A, Katayama M, Handa N, et al: Intramuscular transplantation of G-CSF-mobilized CD34(+) cells in patients with critical limb ischemia: a phase I/IIa, multicenter, single-blinded, dose-escalation clinical trial. Stem Cells, 27: 2857—2864, 2009.
8) Levine AJ, Puzio-Kuter AM: The control of the metabolic switch in cancers by oncogenes and tumor suppressor genes. Science, 330: 1340—1344, 2010.
9) Semenza GL: Hydroxylation of HIF-1: oxygen sensing at the molecular level. Physiology (Bethesda), 19: 176—182, 2004.
10) Lu H, Dalgard CL, Mohyeldin A, et al: Reversible inactivation of HIF-1 prolyl hydroxylases allows cell metabolism to control basal HIF-1. J Biol Chem, 280: 41928—41939, 2005.
11) Akita T, Murohara T, Ikeda H, et al: Hypoxic preconditioning augments efficacy of human endothelial progenitor cells for therapeutic neovascularization. Lab Invest, 83: 65—73, 2003.
12) Ivan M, Haberberger T, Gervasi DC, et al: Biochemical purification and pharmacological inhibition of a mammalian prolyl hydroxylase acting on hypoxia-inducible factor. Proc Natl Acad Sci U S A, 99: 13459—13464, 2002.
13) Aisaki K, Kanno H, Oyaizu N, et al: Apoptotic changes precede mitochondrial dysfunction in red cell-type pyruvate kinase mutant mouse erythroleukemia cell lines. Jpn J Cancer Res, 91: 171—179, 1999.
14) Oyama H, Minakami S: Studies on erythrocyte glycolysis. V. Change of the glycolytic intermediate pattern of reticulocytes during maturation. J Biochem, 61: 103—107, 1967.
15) Aicher A, Zeiher AM, Dimmeler S: Mobilizing endothelial progenitor cells. Hypertension, 45: 321—325, 2005.
16) Krenning G, van Luyn MJ, Harmsen MC: Endothelial progenitor cell-based neovascularization: implications for therapy. Trends Mol Med, 15: 180—189, 2009.

17) Plouffe BD, Kniazeva T, Mayer JE, et al: Development of microfluidics as endothelial progenitor cell capture technology for cardiovascular tissue engineering and diagnostic medicine. FASEB J, 23: 3309—3314, 2009.
18) Lee MS, Moon EJ, Lee SW, et al: Angiogenic activity of pyruvic acid in in vivo and in vitro angiogenesis models. Cancer Res, 61: 3290—3293, 2001.
19) Di Santo S, Yang Z, Wyler von Ballmoos M, et al: Novel cell-free strategy for therapeutic angiogenesis: in vitro generated conditioned medium can replace progenitor cell transplantation. PLoS One, 4: e5643, 2009.
20) Powell RJ, Comerota AJ, Berceli SA, et al: Interim analysis results from the RESTORE-CLI, a randomized, double-blind multicenter phase II trial comparing expanded autologous bone marrow-derived tissue repair cells and placebo in patients with critical limb ischemia. J Vasc Surg, 2011 [Epub ahead of print].
21) Dennis JE, Esterly K, Awadallah A, et al: Clinical-scale expansion of a mixed population of bone-marrow-derived stem and progenitor cells for potential use in bone-tissue regeneration. Stem Cells, 25: 2575—2582, 2007.

ピルビン酸添加による骨髄単核球における血管内皮増殖因子の発現増強を目指した短期培養法の研究

菅野　仁[1)2)]　入部　雄司[1)]　青木　貴子[2)]　小倉　浩美[1)]　藤井　寿一[1)]
[1)]東京女子医科大学輸血・細胞プロセシング科
[2)]東京女子医科大学附属遺伝子医療センター

要旨：

血管内皮前駆細胞（EPC）を用いた血管再生療法は血管バイパス形成術や血管内膜切除術の適応とならない重症虚血肢に対する治療オプションとして近年脚光を浴びている．骨髄からのEPC動員や局所におけるEPCの血管内皮細胞への分化には血管内皮増殖因子（VEGF）が重要な役割を果たしていることから，今回我々はマウス骨髄単核球（BMMNC）を用いて *VEGF* 遺伝子発現の増強およびVEGF分泌量の増加を図るための新規培養法の開発を目指し，以下の実験を行なった．

VEGFは低酸素下で転写因子HIF-1が安定化することで誘導される．その背景にはプロリル水酸化酵素（HIF-PH）の活性がピルビン酸により阻害されることが明らかになっている．ピルビン酸がBMMNCにおけるVEGF発現を増強することが期待されたため，マウスBMMNCのピルビン酸添加培養を行なった．EPC表面マーカーである$CD31^+$/$CD34^+$二重陽性細胞は5mMピルビン酸により最も高くなり，VEGF遺伝子発現量は2日間の培養により培養前の27.8倍にまで達した．さらに培養液中VEGF濃度は5mMピルビン酸，4日間培養にて有意な上昇を認めた．

ピルビン酸は細胞のエネルギー代謝上必須の有機酸であり，無害で安価のため，今回開発したEPC体外増幅法は今後治療的血管新生への応用が期待出来る．

キーワード：
重症虚血肢，再生医療，血管内皮細胞増殖因子（VEGF），血管内皮前駆細胞

Journal Web Site: http://www.jstmct.or.jp/jstmct/

J Clin Immunol (2011) 31:762–772
DOI 10.1007/s10875-011-9560-4

Decreased Expression in Nuclear Factor-κB Essential Modulator Due to a Novel Splice-Site Mutation Causes X-linked Ectodermal Dysplasia with Immunodeficiency

Shuhei Karakawa · Satoshi Okada · Miyuki Tsumura · Yoko Mizoguchi · Norioki Ohno · Shin'ichiro Yasunaga · Motoaki Ohtsubo · Tomoki Kawai · Ryuta Nishikomori · Takemasa Sakaguchi · Yoshihiro Takihara · Masao Kobayashi

Received: 6 March 2011 / Accepted: 14 June 2011 / Published online: 1 July 2011

Abstract X-linked ectodermal dysplasia with immunodeficiency (XL-ED-ID) is caused by hypomorphic mutations in *NEMO*, which encodes nuclear factor-kappaB (NF-κB) essential modulator. We identified a novel mutation, 769−1 G>C, at the splicing acceptor site of exon 7 in *NEMO* in a Japanese patient with XL-ED-ID. Although various abnormally spliced NEMO messenger RNAs (mRNAs) were observed, a small amount of wild-type (WT) mRNA was also identified. Decreased NEMO protein expression was detected in various lineages of leukocytes. Although one abnormally spliced NEMO protein showed residual NF-κB transcription activity, it did not seem to exert a dominant-negative effect against WT-NEMO activity. $CD4^+$ T cell proliferation was impaired in response to measles and mumps, but not rubella. These results were consistent with the clinical and laboratory findings of the patient, suggesting the functional importance of NEMO against specific viral infections. The 769−1 G>C mutation is responsible for decreased WT-NEMO protein expression, resulting in the development of XL-ED-ID.

Keywords NEMO · XL-ED-ID · *IKBKG* · splice-site mutation · measles

Introduction

X-linked ectodermal dysplasia with immunodeficiency (XL-ED-ID) is an X-linked recessive disease which is characterized by missing or malformed teeth, coarse hair, dry skin, hypohidrosis, and immunodeficiency. It is reportedly caused by mutations in the inhibitor of a kappa light polypeptide gene enhancer in B cells, kinase gamma (*IKBKG*), also called nuclear factor-kappaB (NF-κB) essential modulator (*NEMO*) [1]. NEMO is a subunit of the inhibitor of kappaB (IκB) kinase (IKK) complex and plays pivotal regulatory roles in NF-κB signaling pathways. The IKK complex is activated via NEMO in response to stimulation of a wide range of receptors, including Toll like receptors, CD40, proinflammatory cytokine receptors, ectodysplasin receptor, and receptor activator of NF-κB [2–4]. The activated IKK complex induces ubiquitin-mediated proteasomal degradation of IκB, resulting in translocation of NF-κB dimers from the cytoplasm to the nucleus. Subsequently, NF-κB binds to specific κB sites and regulates target gene transcription, activating downstream

Electronic supplementary material The online version of this article (doi:10.1007/s10875-011-9560-4) contains supplementary material, which is available to authorized users.

S. Karakawa · S. Okada (✉) · M. Tsumura · Y. Mizoguchi · N. Ohno · M. Kobayashi
Department of Pediatrics,
Hiroshima University Graduate School of Biomedical Sciences,
1-2-3 Kasumi, Minami-ku,
Hiroshima 734-8551, Japan
e-mail: s-okada@pg8.so-net.ne.jp

S. Yasunaga · M. Ohtsubo · Y. Takihara
Department of Stem Cell Biology, Research Institute for Radiation Biology and Medicine, Hiroshima University,
Hiroshima, Japan

T. Kawai · R. Nishikomori
Department of Pediatrics,
Kyoto University Graduate School of Medicine,
Kyoto, Japan

T. Sakaguchi
Department of Virology,
Hiroshima University Graduate School of Biomedical Sciences,
Hiroshima, Japan

processes involved in inflammation, immunity, cell proliferation, apoptosis, ectodermal formation, and osteogenesis.

Patients with XL-ED-ID are susceptible to multiple and severe bacterial infections of the respiratory and gastrointestinal tracts, skin, soft tissues and bones, together with meningitis and septicemia, from the early stage of infancy [5, 6]. In addition to recurrent severe pyogenic infections, patients also show susceptibility to mycobacterial infections. Although viral infections are not thought to be representative symptoms, some patients suffer from viral infections, e.g., cytomegalovirus (CMV), molluscum contagiosum virus, human papilloma virus, and herpes simplex virus [6, 7]. The immunological abnormalities in the patient with XL-ED-ID are characterized by dysregulated immunoglobulin synthesis or hyperimmunogloblin M (hyper-IgM) syndrome, impaired specific antibody production, defective natural killer (NK) cell activity, and poor proinflammatory cytokine production in response to physiological stimuli. Thus, in patients with XL-ED-ID, responses to various stimuli such as lipopolysaccharide (LPS), interleukin-1 (IL-1), IL-12, IL-18, tumor necrosis factor alpha (TNF-α), and CD40 ligand (CD40L) are impaired [8–11].

Male subjects inheriting large deletions, frameshifts, or other amorphic mutations in *IKBKG* die in utero, indicating that NEMO is essential for development in humans. The mutations in patients with XL-ED-ID are hypomorphic and these mutations impair, but do not abolish NF-κB signaling, thus resulting in distinct clinical and immunological phenotypes.

We identified a novel splice-site mutation, 769−1 G>C, in *IKBKG* in a Japanese boy with XL-ED-ID. This splice-site mutation was shown to produce not only various types of abnormal messenger RNAs (mRNAs), but also low expression of wild-type (WT) mRNA. The expression of WT and abnormal NEMO proteins was also confirmed to be at decreased level in this patient. The decreased expression of NEMO protein is suspected to play an important role in the development of XL-ED-ID.

Methods

Case Report

The patient was a 12-year-old male. He presented with mild mental retardation, conical-shaped teeth, and hypodontia. Hypohidrosis and alopecia were not observed. Similar symptoms were not observed in his family members. He had suffered from recurrent bacterial infections, e.g., three episodes of bacterial meningitis (at 18, 27, and 28 months of age; the pathogenic bacteria isolated from cerebrospinal fluid was *Streptococcus pneumoniae* in the first and third episodes and was unknown in the second episode), recurrent episodes of pneumonia, cellulitis (at 4 years of age; the pathogenic bacteria was unidentified), left knee arthritis (8 years of age, *S. pneumoniae*), and osteomyelitis (12 years old; the pathogenic bacteria was unknown). Furthermore, the patient had also suffered from measles despite receiving a measles vaccination.

The white blood cell and neutrophil counts were both slightly decreased (Table I). The percentage of CD3, CD4, CD8, and CD16/56 in lymphocytes was within the normal range. However, a mild decrease was noted in the $CD19^+$ B cell population. The serum immunoglobulin levels and complement levels were within normal ranges. The production of specific antibodies against *S. pneumoniae* and measles were impaired despite having a history of infections and vaccinations. The specific antibody against *S. pneumoniae* was measured by ELISA and included the antigens of 23 serotypes. He had been vaccinated once with Pneumovax®23 at the age of 9. Furthermore, the specific antibody against the mumps virus was not produced, although the patient was administered the mumps vaccination. However, specific antibodies against CMV, Epstein–Barr virus, Varicella zoster virus, and rubella virus were normally developed. The abdominal ultrasonography examination revealed that the patient's spleen was of normal size. The parents of the patient did not present with immunodeficiency or incontinentia pigmenti.

We obtained blood samples from the patient and healthy adult controls after obtaining informed consent. This study was approved by the Ethics Committee/Internal Review Board of Hiroshima University.

Molecular Genetics

Total RNA was extracted from peripheral blood mononuclear cells (PBMCs). Subsequently, complementary DNA (cDNA) was synthesized by reverse transcription. Polymerase chain reaction (PCR) was performed using primer set 1 (which spans the entire coding region of *IKBKG*, see Supplementary Table) and an Expand Long PCR system (Roche Diagnostics, Germany). The PCR products were sequenced using primer sets 1 and 2. Genomic DNA was extracted from peripheral blood leukocytes and buccal mucosa. Sequence analysis was performed as described previously [12]. In order to investigate the splicing pattern of exon 7, PCR was performed using peripheral blood leukocyte cDNA and primer set 3. The PCR products were cloned into the pGEM-T Easy vector (Promega, USA), and individual alleles were sequenced.

To generate WT and mutant *IKBKG* plasmids, cDNA was synthesized from the patient's PBMCs. PCR was performed using KOD PCR system (TOYOBO, Japan) and primer set 4 (F and R), which includes *Hin*dIII and *Bam*HI sites at the 5′- and 3′-end, respectively, and eliminates the stop codon of *IKBKG*. The PCR products were cloned into the pGEM-

Table I Laboratory data

			RR			Negative range
Leukocyte fraction				Specific antibody		
WBC	5,390	/μl	6,000–10,000	*S. pneumoniae*	Negative	Negative
Neut	1,024	/μl	3,300–7,500	Measles	<8	<8
Ly	3,719	/μl	1,200–4,000	Rubella	>128	<2
Mo	215	/μl	200–950	VZV IgG	40	<10
Eo	377	/μl	0–600	Mumps	<2	<2
Lymphocyte fraction				JEV	<4	<4
CD3	72	%	52–78	CMV IgG	20	<4
CD19	5	%	8–24	EBV VCA IgG	20	<10
CD16/56	21	%	6–27	EBV VCA IgM	<10	<10
CD3/4	38	%	25–48	EBNA	<10	<10
CD3/8	19	%	9–35	Polio type 1, 2, 3	<4	<4
Immunobiochemistry				Pertussis	10	<10
IgG	966	mg/dl	816–1,342	Others		
IgA	292	mg/dl	154-336	NK cell cytotoxicity	6	15–40%
IgM	76	mg/dl	62-103	LTT	Positive	
IgE	54	mg/dl	<100			
CH50	31.2	U/ml	25–48			
C3	97	mg/dl	65–135			
C4	19	mg/dl	13–40			

VZV Varicella zoster virus, *JEV* Japanese encephalitis virus, *CMV* cytomegalovirus, *EBV* Epstein–Barr virus, *EBNA* EBV nuclear antigen, *LTT* lymphocyte transformation test, *RR* reference range

T Easy vector. To generate the construct with a frameshift mutation that produced a premature stop codon, we repeated the PCR to eliminate the original stop codon using primer set 4 (F and R2). These fragments were cloned into P3xFlag-CMV-14 expression vector (Invitrogen, USA) using the *Hin*dIII and *Bam*HI sites.

Reporter Assay

WT and mutant constructs (2 ng per well), IgK-cona-Luc (provided by S. Yamaoka), and pRL-TK (TOYO-B-Net, Japan) were transfected into the NEMO null rat fibroblast cells (provided by S. Yamaoka) using FuGENE HD Transfection Reagent (Roche). We used WT and each of the mutants (1 ng per well, respectively) for co-transfection experiments. At 24 h after transfection, the cells were stimulated with 15 ng/ml LPS (Sigma-Aldrich, USA) for 4 h. Then, cells were subjected to a luciferase assay using the PicaGene Dual Luciferase Assay Kit (TOYO-B-NET). Experiments were done in triplicate and the firefly luciferase activity was normalized to the renilla activity.

Western Blot Analysis

The total proteins from EB virus-transformed B cells (EBV-B cells) were subjected to an immunoblot analysis. We used a mouse anti-NEMO antibody (BD Bioscience, USA) and an anti-flag antibody (Sigma-Aldrich) to detect the NEMO protein and an anti-β-actin antibody (Sigma-Aldrich) as a loading control.

Electrophoretic Mobility Shift Assay

EBV-B cells were stimulated with 10 ng/ml IL-1β (Sigma-Aldrich) for 30 min and subjected to nuclear extraction. We incubated 10 μg of nuclear extract with ^{32}P-labeled (α-dATP) NF-κB probe. The NF-κB double-stranded oligonucleotides corresponding to a NF-κB-binding site consensus sequence 5′-GAT CAT GGG GAA TCC CCA-3′ were used as a NF-κB probe [13].

Flow Cytometry and Carboxyfluorescein Diacetate Succinimidyl Ester Analyses

Flow cytometry analysis of intracellular NEMO protein was performed using the previously reported method [12]. The cells were stained for the following lineage markers after staining for NEMO: CD3, CD14, CD19, and CD56 (BD Bioscience). For CD40L stimulation, PBMCs were cultured with recombinant soluble human CD40L (rCD40L; 2.5 μg/ml; PeproTech Inc, USA) for 48 h and then stained for FCE2 (CD23), ICAM-1 (CD54), Fas (CD95), and CD19

(BD Bioscience). For memory B cell analysis, PBMCs were stained with APC-conjugated anti-CD19, PE-conjugated anti-CD27, and FITC-conjugated anti-IgD antibodies (BD Biosciences). Three-color analysis was carried out by gating on CD19-APC-positive B cells.

For the preparation of measles virus-infected cell lysates (measles lysates), Vero cells were infected with measles virus (the Edmonston strain). Measles lysates were prepared from the cells by clarification with a low-speed centrifugation. The PBMCs from the patient and five healthy adult controls (all were approximately 20 years of age and had developed specific antibodies against measles, rubella, and mumps) were incubated with carboxyfluorescein diacetate succinimidyl ester (CFSE) (Sigma-Aldrich) at a concentration of 0.05 mM [14, 15]. The cells were cultured for 7 days in RPMI-1640 (Sigma-Aldrich) containing 10% AB human serum supplemented with 1 or 3 μg/ml phytohemagglutinin (PHA) (Sigma-Aldrich), 1 or 10 μg/ml measles lysates, 1 or 5 μg/ml rubella lysates (Meridian Life Science, USA), and 1 or 10 μg/ml mumps lysate (Fitzgerald, USA). These cells were stained with APC-conjugated anti-CD4 antibodies (BD Biosciences) and subjected to a flow cytometry analysis.

Cytokine Measurements

We used PBMCs from the patient and four age-matched healthy adult controls (aged 20 years). $CD14^+$ cells were purified from PBMCs using by magnetic sorting (BD Biosciences). The purity levels of $CD14^+$ cells were more than 90%. The $CD14^+$ cells were cultured for 48 h with the addition of 100 U/ml LPS, and the concentration of TNF-α in supernatant was measured in duplicate by Luminex.

Results

A Novel Splice-Site Mutation in *IKBKG* Results in Various Abnormal Splicing Products

High molecular weight DNA was extracted from both the peripheral blood samples and buccal mucosa, and the exons and flanking introns of *IKBKG* were amplified by PCR and sequenced. We identified a novel hemizygous single base-pair G-to-C substitution at nucleotide 769 (−1), 769−1 G>C, of intron 6 in *IKBKG* in the peripheral blood samples (Fig. 1a). The same mutation was also identified in genomic DNA from buccal mucosa, suggesting that this mutation is a germ-line mutation (data not shown). We could not examine the patient's parents and siblings because we could not obtain consent from these family members. Thus, we excluded the possibility that this mutation was a common or irrelevant polymorphism by sequencing 214 healthy

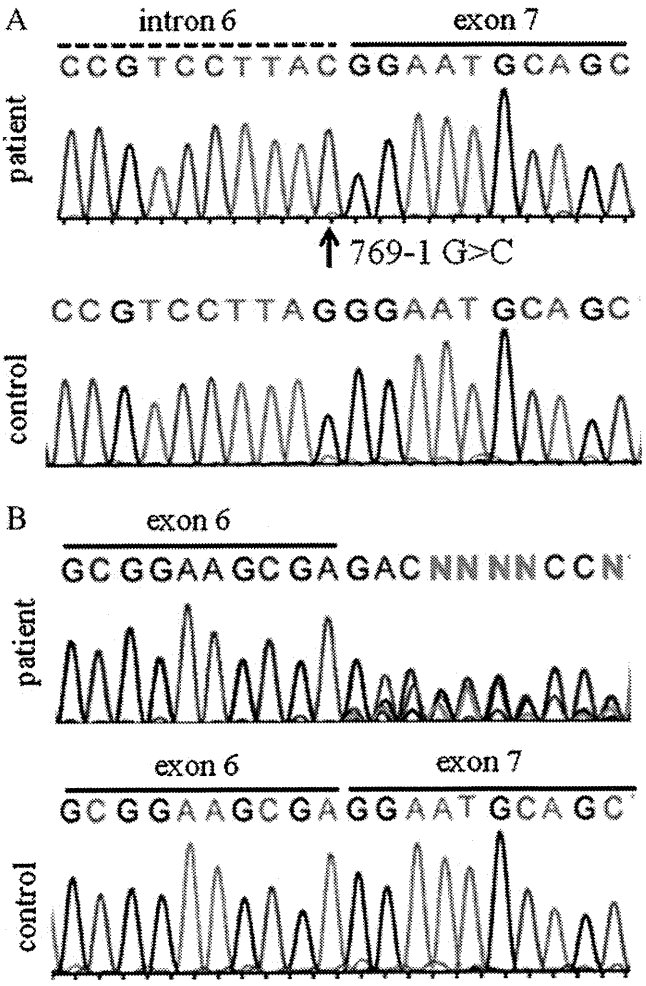

Fig. 1 Sequence analysis. **a** Genomic DNA from the patient and healthy controls were amplified by PCR and the products were analyzed by Sanger sequencing. A novel hemizygous single base-pair G-to-C substitution at nucleotide 769 (−1), 769−1 G>C, was identified in IVS6 of *IKBKG*. **b** Total RNA was extracted from peripheral blood mononuclear cells and cDNA was synthesized by reverse transcription. PCR was performed using primers that spanned the entire coding region of *IKBKG*. The presence of various abnormal splicing variants was predicted in the patient

individuals, including 58 Japanese individuals. A splice junction sequence is highly conserved in eukaryotic cells, which is generally known as a GT-AG rule [16, 17]. Since 769−1 G>C is involved in the highly conserved splicing acceptor site, we analyzed the impact of this mutation on NEMO mRNA splicing. As shown in Fig. 1b, the presence of various abnormal splicing variants was predicted.

In order to investigate the effect of this mutation on splicing, we performed PCR on cDNA with primers which span exons 6 and 7 of *IKBKG*. PCR products were cloned into pGEM-T Easy vector and were subjected to sequence analysis. A sequence analysis of 24 clones demonstrated that 7 clones were derived from normal splicing and the other 17 clones from various abnormal splicing events

(Fig. 2a). Although these abnormal splicing patterns contained insertions and/or deletions in various locations, the major mutant patterns were a 171-bp insertion (+171-NEMO) and 64-bp insertion (+64-NEMO) at the splice acceptor site of exon 7. Among the 17 clones from the abnormal splicing, 13 clones had in-frame changes resulting in large conformational changes of the NEMO protein, and 4 clones (+64-NEMO) were a frameshift change resulting in the premature termination of protein translation (Fig. 2a). The ratio of WT and mutants was similar in PHA- and IL-2-induced T cell blasts which were obtained on the same day (Fig. 2b). We also collected blood samples from the patient on other days, including 1 day the patient was experiencing fever. The ratio of WT to mutant differed in these later samples, compared to those in the initial analysis. In these later timepoints, the ratio of WT was decreased to 5% or 18%, suggesting that the ratio of WT mRNA varies in the patient over time (Fig. 2c, d). To examine whether these splicing variants were also observed in healthy individuals, we tested five healthy individuals and did not find any of the variants found in the patient (representative sequences are shown in Fig. 1b). Altogether, these results suggest that the 769−1 G>C mutation in *IKBKG* is responsible for various abnormal NEMO splicing products.

NEMO Protein Expression Is Decreased in the Patient

In order to examine the effect of the *IKBKG* mutation at the protein level, we analyzed the expression of intracellular NEMO by a flow cytometry analysis. The expression of the NEMO protein in the patient was lower than that in healthy controls in terms of CD3, CD4, CD8, CD56, CD14, and CD19-positive cells (Fig. 3a). Next, we performed an

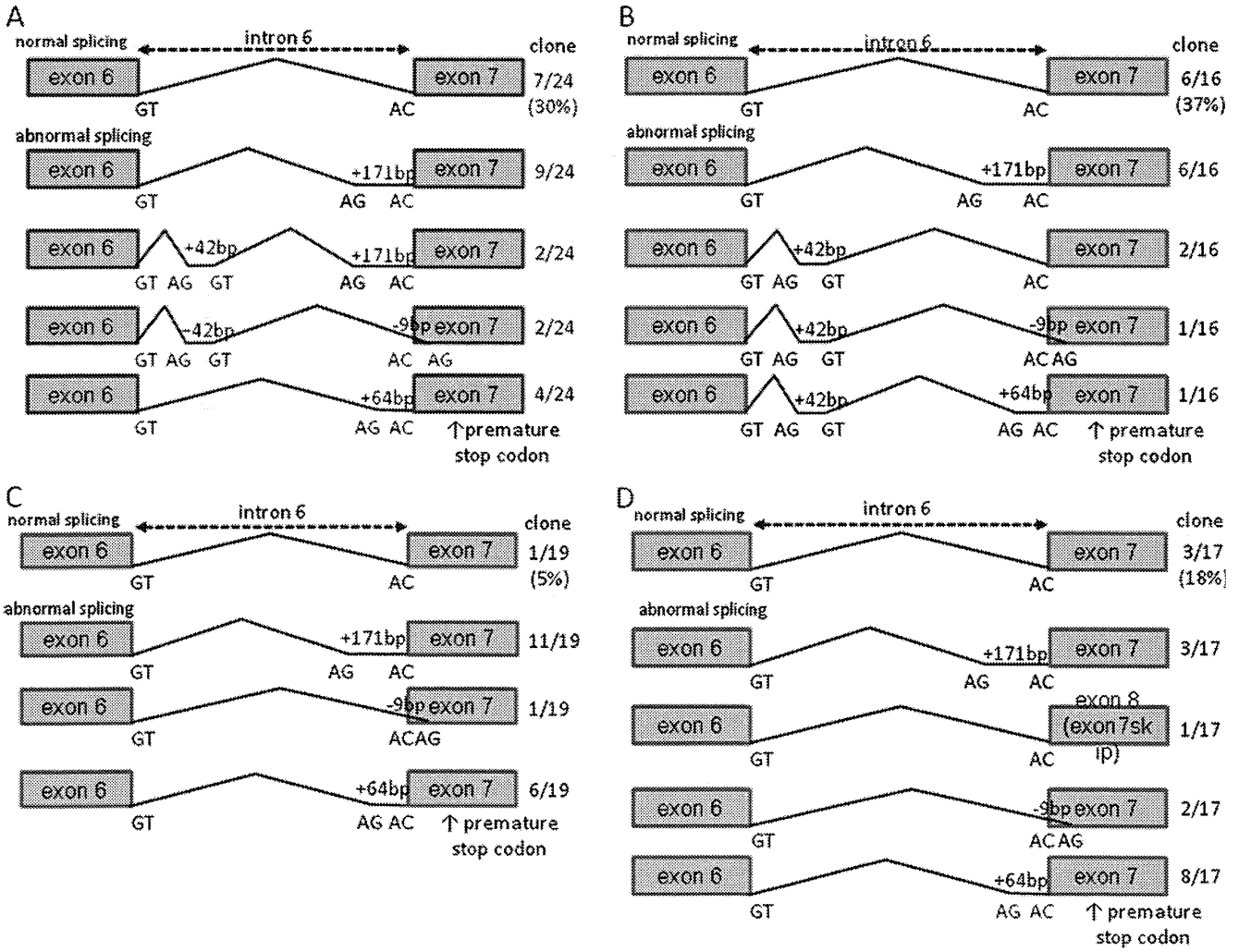

Fig. 2 Cloning analysis. **a** PCR products were cloned into the pGEM-T Easy vector and were subjected to sequence analysis. The splice pattern and the observed number of each clone are shown. The same studies were performed using PHA- and IL-2-induced T cell blasts which were obtained the same day (**b**), PBMCs obtained another day (**c**), and PBMCs obtained on the day the patient was experiencing fever (**d**). The splice pattern and the ratio of WT or mutant variants were different based on the timing of blood collection

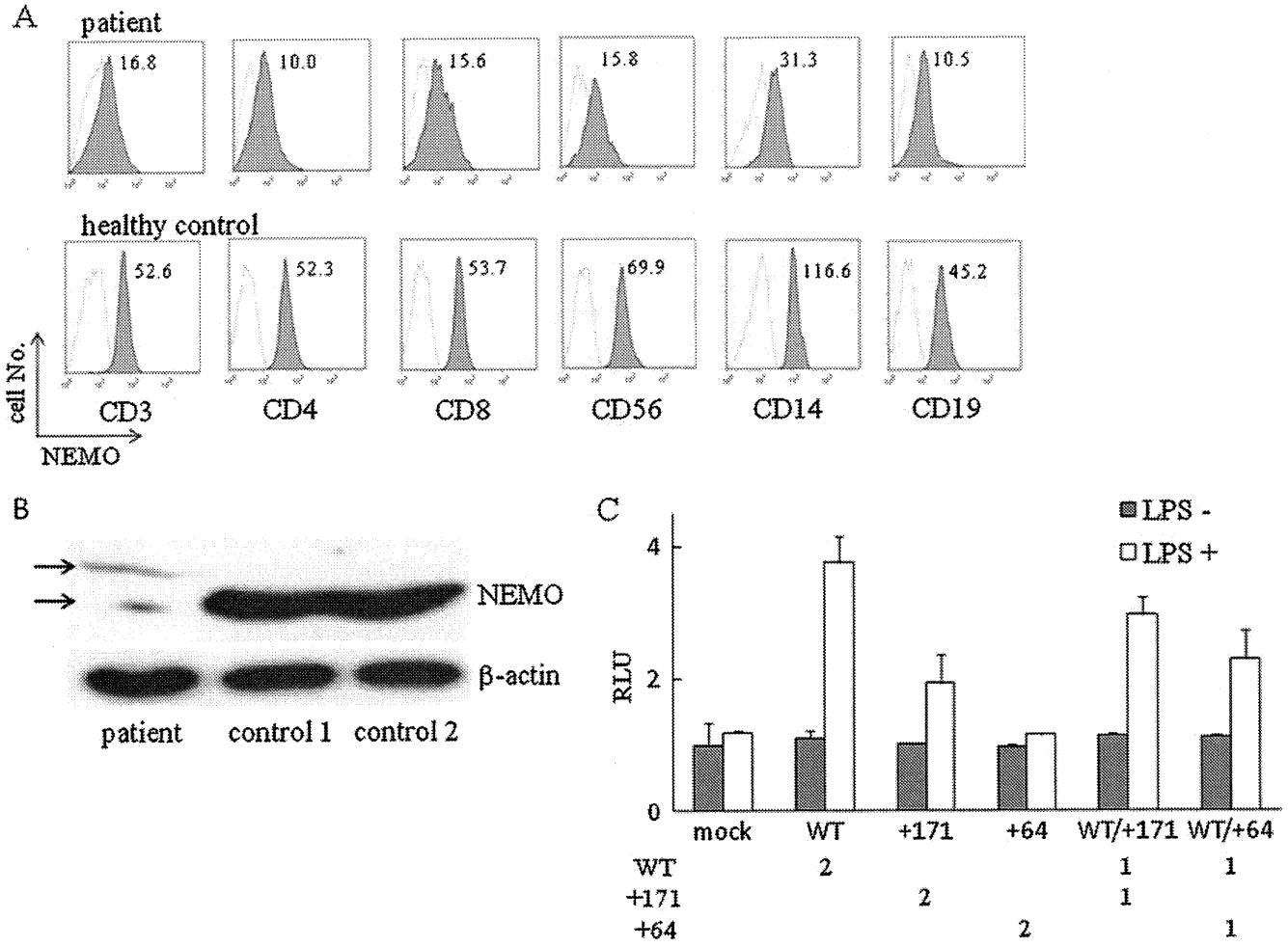

Fig. 3 Analysis of NEMO protein expression and reporter assay. **a** Expression of intracellular NEMO protein from the patient was decreased in various lineages of leukocytes. The geometrical mean fluorescence intensity of NEMO is shown in the FACS profile. **b** EBV-B cells from the patient showed decreased levels of NEMO protein expression. The *upper arrow* shows the band derived from +171-NEMO (approximately 57 kDa), while the *lower arrow* shows WT-NEMO (50 kDa). EBV-B cells in the patient were established from the same blood collection as was used for the cloning analysis of Fig. 2a. **c** WT-, +171-, and +64-NEMO were transfected into NEMO null cells, and NF-κB activity was measured by luciferase assay. The quantity of plasmids (nanogram) used for transfection is described

immunoblot analysis using EBV-B cells from the patient. As shown in Fig. 3b, two major bands were detected, corresponding to the expected molecular weight of the +171-NEMO mutant (approximately 57 kDa) and the known molecular weight of WT-NEMO (50 kDa). The results of densitometry revealed that the expression of WT-NEMO protein from the patient was eightfold lower than that from healthy controls. NEMO mutant proteins derived from other abnormally spliced mRNAs were not detected in this assay.

The Mutant NEMO Proteins Show Decreased NF-κB Transcriptional Activity

To further clarify the characteristics of these abnormally spliced mRNAs, we performed transient gene expression experiments specifically focused on the abnormal splicing products, +171- and +64-NEMO. WT and these mutant constructs were transfected into NEMO null cells. The expression of the WT- and +171-NEMO proteins was detected by either anti-NEMO or anti-Flag antibodies (Supplementary Figure). We were unable to detect the expression of the +64-NEMO protein in the transfectants, suggesting that the +64-NEMO protein may be unstable. Then, we examined the impact of these mutants on NF-κB activation using reporter assay. As shown in Fig. 3c, +64-NEMO abolished NF-κB activation in response to LPS stimulation. On the other hand, +171-NEMO displayed residual NF-κB activity. To further clarify the effect of these mutants on the WT protein, we performed a co-transfection experiment. Co-transfection with half of the amount of WT and +171-NEMO (WT/+171) resulted in only 75% of the

NF-κB activity compared to cells transfected with WT-NEMO, while co-transfection with WT and +64-NEMO (WT/+64) resulted in approximately 50% of WT activity. Considering that +64-NEMO is not expressed at the protein level, the 50% NF-κB activity observed here is likely derived from half the amount of WT-NEMO plasmid. On the other hand, +171-NEMO is thought to have residual activity, even after co-transfection with WT-NEMO. This result suggests that these mutants do not seem to exert a dominant-negative effect against WT-NEMO-mediated NF-κB activation. However, we could not completely rule out the negative effect caused by the other abnormally spliced variants, since we examined only two representative variants.

The Functional Activity via NEMO Is Impaired in the Patient

To analyze the functional impairment caused by the NEMO mutation, we examined the CD23, CD56, and CD95 expression on $CD19^+$ B cells, markers of activated B cells, in response to CD40L stimulation. As shown in Fig. 4a, CD54 and CD95 expressions were reduced compared to healthy controls, and CD23 expression was not detected in the patient's B cells, suggesting that activation of B cells was not completely abrogated in the patient, but instead $CD19^+$ B cells from the patient showed weak levels of activation. Therefore, the patient's cells showed partial, but not complete, impairment following CD40L stimulation. Next, we tested TNF-α production in response to LPS stimulation in peripheral blood $CD14^+$ monocytes. As shown in Fig. 4b, $CD14^+$ monocytes from the patient showed a lower level of TNF-α production compared with those from healthy controls. To further clarify the functional defects, we assessed NF-κB DNA-binding ability in response to IL-1β stimulation using EBV-B cells. As shown in Fig. 4c, NF-κB DNA-binding ability was severely impaired, but not abolished, in the patient. Thus, similar to other patients with XL-ED-ID, the patient's cells also showed impairment in response to various stimuli which induce IKK activation.

Memory B Cells Are Decreased in the Patient

The number of $CD27^+$ memory B cells within the $CD19^+$ B cell population was decreased in the patient (6.0%) in comparison to the number observed in healthy controls (30.4±17.8%, $n=10$). A reduced number of $CD27^+$ memory B cells has also been reported in patients with X-linked anhidrotic ectodermal dysplasia with hyper-IgM syndrome (HED-ID) caused by NEMO impairment [18, 19] as well as in a patient with a 5′ untranslated region (UTR) mutation of *IKBKG*, with high levels of IgA [20]. However, as far as we know, a reduction in the memory B cell compartment has not yet been reported in patients with ED-ID. B cells in patients with defect in NF-κB are unable to undergo somatic hypermutation and class switch recombination, resulting in a loss of memory B cells [19, 21, 22]. Although we need to test other patients with ED-ID to confirm this memory B cell phenotype, the diminished memory B cell population may become a common finding not only in patients with HED-ID, but also in patients with an impairment of NEMO.

The Increase in $CD4^+$ T Cell Proliferation Is Impaired for Measles and Mumps Infections

The patient developed measles in spite of having a history of measles vaccination. Furthermore, although specific antibodies against measles and mumps virus were not detected, specific antibodies against CMV, Epstein–Barr virus, Varicella zoster virus, and rubella virus were normal. To clarify the mechanism underlying the impairment of specific antibody production against measles and mumps viruses, we tested the specific T cell response against these viral infections. We analyzed $CD4^+$ T cells using a CFSE proliferation assay according to the method described in a previous report [23]. $CD4^+$ T cells from the patient were unable to proliferate in response to measles lysate and mumps lysate (Fig. 5a, b). On the other hand, they proliferated well in response to PHA and rubella lysate. CFSE is a commonly used and useful tool for analyzing specific T cell response against *Candida*, CMV, measles viruses, and others, and these results suggest that the specific T cell response against measles and mumps virus is impaired in the patient [14, 15, 23]. These findings were compatible with patient's laboratory findings of the impairment of a specific antibody production against measles virus and mumps virus, in spite of having received these vaccinations and having a prior measles infection.

Discussion

We identified a novel hemizygous splice-site mutation in *IKBKG* in a Japanese boy with XL-ED-ID. Both the WT and various abnormally spliced forms of NEMO mRNA were observed in the patient's cells. There are two possibilities which may account for this finding. One is leakage through the splice-site mutation, the other is mosaicism. Leakage through the splice-site mutation has also been described in many human diseases [24–26], including in a patient with a NEMO abnormality who had a splice-site mutation, 1056−1 G>A [27]. Similar to what was observed in our current study, the ratio of WT to mutant NEMO mRNA observed varied with the timing of blood